ISBN: 978-3-95450-249-3 ISSN: 2673-5350 doi: 10.18429/JACoW-IBIC2024-THP51

SPECIALIZED OPTICAL PULSE PICKER FOR BEAM DIAGNOSTICS IN STORAGE RING*

Mingdong Ma, Dongyu Wang, Chuhan Wang, Baogen Sun, Jigang Wang†
National Synchrotron Radiation Laboratory,
University of Science and Technology of China Hefei, China 230029

Abstract

The non-uniformity, longitudinal oscillations, and space charge effects in a multi-bunch filled electron storage ring can lead to significant deviations in the measurement of longitudinal beam parameters. Selecting a single bunch for measurement can effectively improve the measurement accuracy of longitudinal beam parameter, under normal multi-bunch operation mode. This paper introduces an optical pulse selection system based on an RTP crystal Pockels cell, which is controlled by fast electronics and high-voltage electronics, to study the complex longitudinal beam dynamics. By adjusting the driving voltage frequency and trigger delay of the high-voltage driver, precise selection of single pulses in a multi-bunch filling mode can be achieved. Offline calibration experiments have verified the potential feasibility of selecting specific bunches or bunch trains within the multi-bunch operation, which is of great significance for diagnosing longitudinal characteristics and instabilities of the beam in electron storage rings.

INTRODUCTION

The diagnosis of longitudinal beam parameters is crucial for the performance characterization of particle accelerators and the precision of experiments [1]. Longitudinal parameters mainly include the beam energy, energy spread, longitudinal emittance, bunch length, and longitudinal phase space distribution [2-4]. Accurate diagnosis of these parameters aids in understanding and optimizing beam behaviors in accelerators. Among the diagnostic tools, streak cameras have become indispensable due to its high spatio-temporal resolution and sensitivity [5-8]. However, prolonged measurement of longitudinal beam parameters can cause irretrievable damage to the photocathode, MCP, and CCD phosphor screen of the streak camera. Additionally, when performing measurements on individual bunches, stray light from other bunches may leak into the streak camera images, resulting in measurement inaccuracies [9]. Optical pulse selection technology addresses these issues by incorporating a gating structure before the entire longitudinal beam diagnostic system, that is capable of selecting specific bunches within a bunch train. Currently, common approaches include integrating a micromechanical shutter gating technique, external MCP gating, or fast electro-optic shutter gating in front of the streak camera to create the protective gating structure [10-12]. However, these methods face significant challenges in practical applications. Micromechanical shutters typically have low modulation rates and are prone to mechanical inaccuracies, while external MCP gating can introduce timing delays and operational complexity, and fast electro-optic shutters may suffer from limited response times and potential alignment issues. These limitations can lead to the reduction of accuracy and reliability in actual bunched beam measurements.

This paper develops an optical pulse selection system based on an RTP electro-optic crystal Pockels cell, utilizing high-voltage electronics and fast electronics to control the RTP crystal. By finely tuning the RF driving frequency and trigger delay of the high-voltage driver, precise selection of optical pulses is achieved. The extinction ratio of the two polarizers in the system is 5419:1, effectively reducing the optical power input to the streak camera. Additionally, the offline calibration experiment demonstrated the feasibility of the system in achieving selective light pulse extraction at a frequency of 4.533 MHz. This is of significant importance for diagnosing longitudinal characteristics and instabilities of the beam in electron storage rings.

DESCRIPTION OF THE OPTICAL PULSE PICKER

The structure and working principle description of the optical pulse selection system are illustrated in Fig. 1. The system primarily consists of two perpendicular polarizing beam splitters (PBS1 and PBS2), a Pockels cell, a high-voltage driving circuit, a delay signal generator, and a water-cooling unit. The RTP crystal (model: RTP-6-20-AR532-DMP) within the Pockels cell serves as the core optical pulse selection component in this system. It features excellent performance characteristics such as a high electro-optic modulation effect, high damage threshold, low optical loss, and a wide spectral transmission range. These properties enable the RTP crystal to operate stably at specific repetition frequencies, ensuring the precision and reliability of the optical pulse selection system.

The operating principle of the system is based on the Pockels effect, wherein the RTP crystal inside the Pockels cell alters the phase of light passing through it when high voltage is applied. The high-voltage driving circuit, designed in a dual push-pull configuration, is directly connected to the Pockels cell. This circuit applies the appropriate high voltage to the Pockels cell in response to the frequency signals output by the delay signal generator, thereby modulating the phase change of the incident light beam. Through precise adjustments of the Pockels cell, including its orientation and voltage amplitude, the system can accurately control the polarization state and phase shift of the light.

* This work was supported by the National Natural Science Foundation of China under Grant 12075236.
† Corresponding author (email: wangjg@ustc.edu.cn).

ISBN: 978-3-95450-249-3 ISSN: 2673-5350 doi: 10.18429/JACoW-IBIC2024-THP51

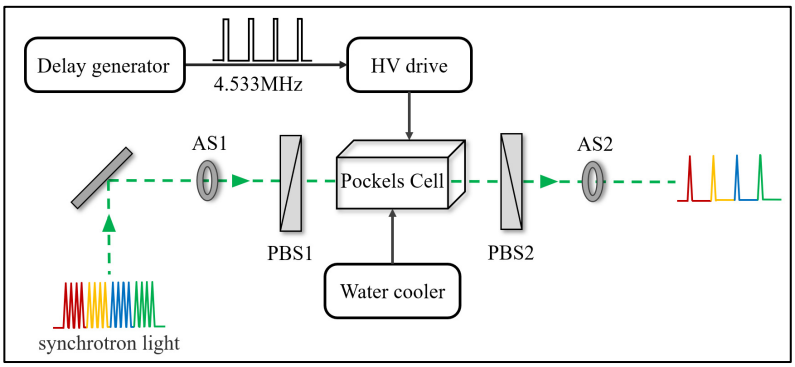

Figure 1: The schematic of the Optical Pulse Picker.

Since the high-voltage driving circuit generates significant heat during operation, the water cooler maintains the temperature inside the Pockels cell at a stable 17°C, to maintain system stability. Indeed, this ensures that the system can operate stably over extended periods under high-frequency and high-load conditions, preventing performance degradation due to temperature increment.

The synchronous light first passes through the polarizer PBS1, becoming linearly polarized light. When the Pockels cell is in its unpowered state (i.e., closed), the phase of the linearly polarized light remains unchanged, preventing it from passing through the orthogonal polarizer PBS2. When the Pockels cell is powered (i.e., open), the phase of the linearly polarized light is altered as light passes through the Pockels cell, allowing it to pass through PBS2. By precisely adjusting the frequency and timing of the voltage applied to the Pockels cell, the system can select synchronous light pulses within a specific time window, achieving precise control and selection of specific optical pulses.

OFFLINE CALIBRATION EXPERIMENTS

To ensure the reliability and accuracy of the system in practical applications, we conducted an offline calibration experiment using a laser to precisely calibrate the optical pulse selection system. The experimental setup shown in the Fig. 2, includes an optical attenuator (ATT), two mirrors (M1 and M2), two apertures (AS1 and AS2), two polarizing beam splitters (PBS1 and PBS2, with orthogonal polarization axes), the Pockels cell, and a photomultiplier tube (PMT).

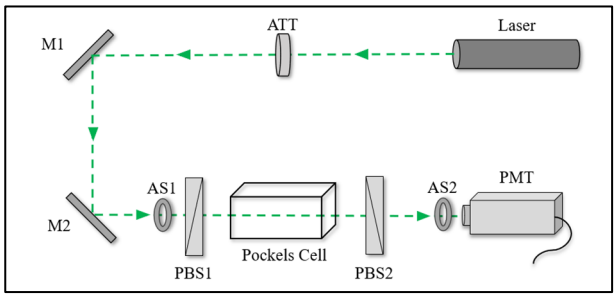

Figure 2: The schematic of offline calibration experimental setup.

The extinction ratio of PBS1 and PBS2, placed orthogonally, was measured using an optical power meter, yielding an extinction ratio of 5419:1. This high extinction ratio ensures that when the Pockels cell is in the closed state, linearly polarized light is effectively blocked. It also improves signal isolation degree during the switching process, reducing crosstalk and signal loss, thereby achieving a higher signal-to-noise ratio.

After that, the experimental optical path was finely aligned. By adjusting the angles and positions of mirrors M1 and M2, the laser beam was accurately directed through the entire optical path. The sizes of apertures AS1 and AS2 were adjusted so that the laser beam spot precisely passed through the aperture openings, reducing stray light interference caused by reflections from optical components that could affect signal detection. Meanwhile, apiece of thin scattering medium is placed in front of the aperture of the Pockels cell to diffuse the laser beam, ensuring more even light distribution. A light screen is positioned behind the polarizing beam splitter PBS2 to observe the patterns formed as the light passes through the crystal. The orientation of the RTP crystal within the Pockels cell is then adjusted while observing the isogyre patterns on the light screen. When a specific isogyre pattern appears as shown in Fig. 3, it indicates that the RTP electro-optic crystal is correctly aligned.

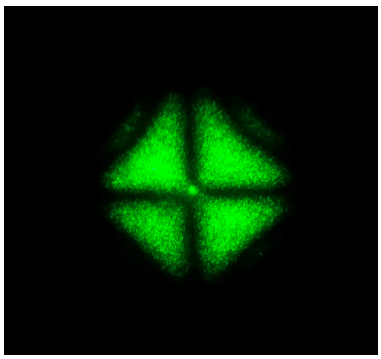

Figure 3: Isogyre patterns image.

After the alignment of the optical path and the adjustment of the crystal orientation are completed, we adjust the pulse delay time on the timing trigger board to control the

ISBN: 978-3-95450-249-3 ISSN: 2673-5350 doi: 10.18429/JACoW-IBIC2024-THP51

timing of the high voltage applied to the Pockels cell. A synchronization optical frequency of 4.533 MHz is input into the signal delay generator, which halves it to a 2.2665 MHz trigger frequency and feeds it into the external trigger input of the pulse timing board. The pulse signal generated by the pulse timing board is formed by subtracting the B-gate signal from the A-gate signal. As shown in the Fig. 4, the A-gate signal has a pulse width of 224 ns, while the B-gate signal has a pulse width of 216 ns, resulting in a Pockels cell control signal with a pulse width of 4 ns and a period of 220 ns, as shown in the Fig. 5. By controlling the timing of the applied voltage, the optical pulse can be selected within a preset time window. Finally, by setting the delay time of the pulse delay generator, the external trigger signal is precisely delayed, achieving a delay of the Pockels cell control signal within 220 ns, thereby verifying the feasibility of the optical pulse selection system for selecting specific bunches.

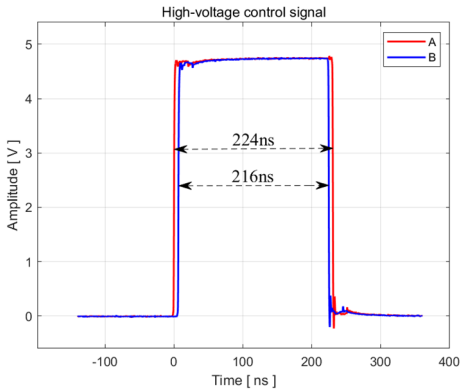

Figure 4: A and B gate signals generated by the pulse timing board.

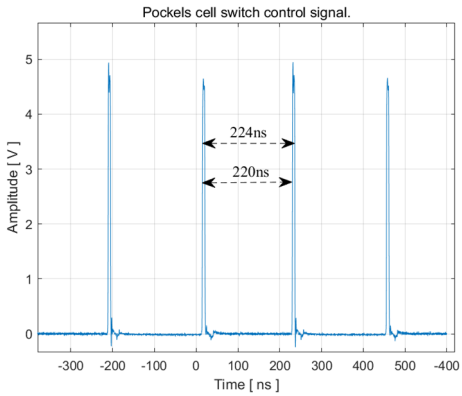

Figure 5: Pockels cell switch control signal with a period of 220 ns and a pulse width of 4 ns.

EXPERIMENTAL RESULTS AND ANALYSIS

Figure 6 shows the signal of a single laser pulse detected by PMT. The solid blue line represents the raw data, while the dashed red line shows the fitted result. The rise time (10-90%) and fall time (90-10%) of the pulse are 2.60 ns and 2.70 ns, respectively, and the full width at half maximum (FWHM) is 3.67 ns, which is shorter than the 4.9 ns bunch spacing in the 45 filling bunch mode of HLS-II. This indicates that the synchronization light from a single bunch can be selected within the switching time of a single pulse.

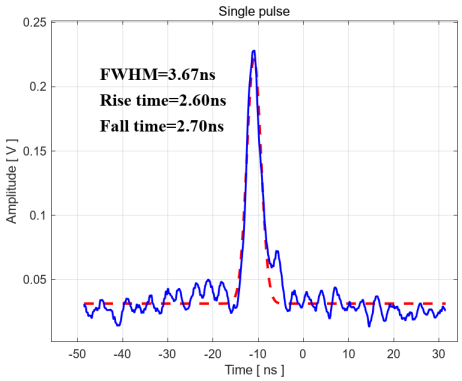

Figure 6: Single pulse output waveform.

Figure 7 shows the laser pulse signals detected by PMT as the delay time of the synchronization light signal (4.533 MHz) is adjusted in 10 ns steps using the signal delay generator. The laser pulse signals also shift by 10 ns in sync with the delayed synchronization light pulses. Eventually, the laser pulse signal delayed by 220 ns completely overlaps with the one delayed by 0 ns, as shown in the Fig. 8. This demonstrates that the system can select any desired bunch within a 0-220 ns window by setting the appropriate delay time on the signal delay generator, verifying the feasibility of selecting specific bunches with this system. For the streak camera system, this capability allows for the observation of specific bunch light pulses while avoiding interference from other bunches, thereby improving the accuracy of the observations. Additionally, it reduces the input time of light pulses, offering protection to the photocathode, MCP, and CCD phosphor screen of the streak camera.

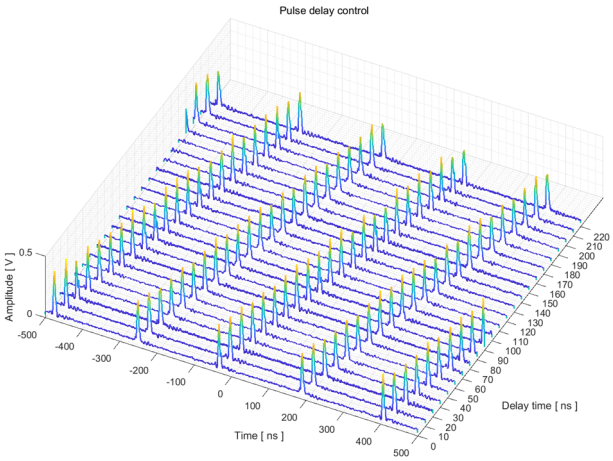

Figure 7: Laser pulse under different delay times.

CONCLUSION

This paper presents the development of a Pockels cell-based optical pulse selection system using an RTP electro-optic crystal. By adjusting the RF driving voltage and

ISBN: 978-3-95450-249-3 ISSN: 2673-5350 doi: 10.18429/JACoW-IBIC2024-THP51

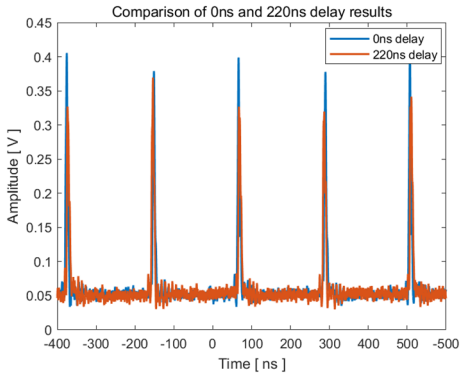

Figure 8: Comparison of 0 ns and 220 ns delay results.

frequency, the system achieves a gating time window with a pulse width of 3.67 ns and a period of 220 ns. Additionally, by setting the signal delay generator, the system can introduce delays within a range of 0-220 ns, demonstrating the feasibility of selecting specific bunches.

The successful implementation of this system is crucial for improving the precision of light pulse selection in storage ring. It allows for the isolation of light from individual bunches, reducing interference from other bunches, and enhancing the accuracy of experimental measurements. This capability is particularly important for applications such as streak cameras, where precise timing and high resolution are essential. This system's ability to control the timing and selection of light pulses contributes to the overall performance and reliability of the storage ring light source, enabling more accurate and detailed studies of beam dynamics and other related physical phenomena and instability mechanisms.

As future work, this system will be applied to HLS-II storage ring to achieve the selection of specific bunches, further enhancing its applicability and demonstrating its effectiveness in a practical setting.

REFERENCES

[1] Y. Zhao *at al*., "Estimations of Longitudinal Impedances Based on Temporal Beam Characteristic Parameter Extraction Method in Storage Ring Light Source", *IEEE Transactions on In-strumentation and Measurement*, vol. 71, p. 1003710, 2022. doi:10.1109/TIM.2022.3160528

[2] T. Lefevre, "Bunch length measurements", Proc. of CERN Accelerator School, Intermediate Level, 2015.

[3] Y. Zhao *at al*., "Characterizations of the longitudinal beam behaviors and impedances measurements at HLS-II", *Measurement*, vol. 187, p. 110280, 2022. doi:10.1016/j.measurement.2021.110280

[4] Y. Zhao *at al*., "Observation and Analysis of Island Phenomenon in the Storage Ring Light Source", in *proc. IBIC2021*, Pohang, Rep. of Korea, 2021, paper WEPP06, pp. 373-376. doi:10.18429/JACoW-IBIC2021-WEPP06

[5] K. Scheidt, "Review of streak cameras for accelerators: features, applications and results", in *proceedings of the European Particle Accelerator Conference*, Vienna, Austria, 2000, pp. 182-186.

[6] A.H. Lumpkin, "The next generation of RF FEL (free electron laser) diagnostics: synchroscan and dual-sweep streak camera techniques", *Nucl. Instrum. Methods Phys. Res. A*, vol. 304, 1991, pp. 31-36. doi:10.1016/0168-9002(91)90815-8

[7] Y. Zhao *at al*., "Method for solving bunch head-tail overlapping in HLS-II using a new trigger scanning module of streak-camera measurement system", *Measurement*, vol. 220, 113344, 2023. doi:10.1016/j.measurement.2023.113344

[8] Y. Zhao *at al*., "Application and Development of the Streak Camera Measurement System at HLS-II", in *proceedings of IPAC2021*, Campinas, Brazil, 2021, pp. 1942-1944. DOI:10.18429/JACoW-IPAC2021-TUPAB222

[9] W. Cheng, "Streak-camera measurements with high currents in pep-ii and variable optics in spear3", SLAC National Accelerator Lab., Menlo Park, CA (United States), 2008.

[10] M. Bergher, "Measurements on the coherent synchrotron radiation effects in surf iii beam", *Nucl. Instrum. Methods Phys. Res., Sect. A*, vol. 492, pp. 464-482, 2002. doi:10.1016/S0168-9002(02)01354-2

[11] J. Hinkson *at al*., "Commissioning of the advanced light source dualaxis streak camera" in *proceedings of the 1997 Particle Accelerator Conference*, vol. 1, 1997, pp. 775-777. doi:10.1109/PAC.1997.749833

[12] J. Corbett *at al*., "Visible light diagnostics at spear3" in *AIP Conf. Proc.* vol. 1234, 2010, pp. 637-640. doi:10.1063/1.3463286